Deep Learning Based Hyperspectral Images Analysis for Shrimp Contaminated Detection

Minh-Hieu Nguyen[1], Xuan-Huyen Nguyen-Thi[1], Cong-Nguyen Pham[1], Ngoc C. Lê[2], and Huy-Dung Han[1(✉)]

[1] Electronics and Computer Engineering Department, School of Electronics and Telecommunications, Hanoi University of Science and Technology, Hanoi, Vietnam
dung.hanhuy@hust.edu.vn

[2] School of Applied Mathematics and Informatics, Hanoi University of Science and Technology, Hanoi, Vietnam

Abstract. In this paper, a deep learning based hyperspectral image analysis for detecting contaminated shrimp is proposed. The ability of distinguishing shrimps into two classes: clean and contaminated shrimps is visualized by t-distributed Stochastic Neighbor Embedding (t-SNE) using spectral feature data. Using only some small data set of hyperspectral images of shrimps, a simple processing technique is applied to generate enough data for training a deep neural network (DNN) with high reliability. Our results attain the accuracy of 98% and F1-score over 94%. This works confirms that with only few data samples, Hyperspectral Imaging processing technique together with DNN can be used to classify abnormality in agricultural productions like shrimp.

Keywords: Hyperspectral Imaging · Abnormality classification · t-SNE · Deep neural network

1 Introduction

Recently, Hyperspectral Imaging/Image (HSI) shows its potential in many sectors such as medical applications, remote sensing imagery or food processing [2–6]. Employing capability of taking images of multiple wavelength bands, including the visible and near-infrared region (VNIR), the HSI system can provide much higher details and extra information compare to conventional RGB (Red Green Blue) images [2]. In HSI, each pixel of the image contains spectral information representing the electromagnetic strength of a narrow wavelength range reflected from the object beamed under a full spectrum light. The wavelength is added as a third dimension to the two-dimensional spatial image, producing a three-dimensional data cube [3]. Thanks to the expanded wavelength range in HSI data cube, HSI captures richer information invisible to the human

N.-S. Vo and V.-P. Hoang (Eds.): INISCOM 2020, LNICST 334, pp. 195–205, 2020.
https://doi.org/10.1007/978-3-030-63083-6_15

eyes, enabling possibilities of data computation and analysis [7]. The rich information in HSI data cube also opens plethora of new applications.

In a report of the U.S. Food and Drug Administration (FDA)[1] in year 2019, three out of the 85 (3.5%) total seafood entry line refusals were of shrimp for reasons related to banned antibiotics. Contaminated shrimp is a big trouble to Vietnamese export seafood sector at the moment. There are several impurities such as agar (jelly-like) or chemical materials like veterinary drug residues. Therefore, the detection of impurities in shrimps is a necessary task to protect health of consumers, to prevent contaminated shrimps from the sources, to ensure the quality and the reputation of Vietnamese seafood production. This work investigates the shrimps suffering from being injected contaminated substance for the purpose of increasing shrimps' weight. To our best knowledge, the problem of classifying clean and contaminated shrimps have not been addressed before in Vietnam.

In this research, HSI of is utilized for shrimps contaminated by unexpected substance detection. The used HSI photography provides detailed spectral data of the shrimps in visible and near-infrared region (VNIR) [7]. The SPECIM FX camera provides 224 spectra spreading from 400 nm to 1000 nm for each pixel of a shrimp image. With pushbroom line scanning mode, the target shrimp is scanned one spatial line at a time and all spectral data from that line is acquired simultaneously. By collecting the unique and detailed spectral information of shrimps, HSI could reveal different materials and physical characteristics. Therefore, the clean shrimps and contaminated shrimps can be classified. Data augmentation by t-Distributed Stochastic Neighbor Embedding (t-SNE) technique has shown that it is possible to classify the two types of shrimps. Training based DNN technique is applied to the collected HSI data and shows the capability of distinguishing clean shrimps and contaminated shrimps with high accuracy.

In the next section, we will summary some works related to the issue. The system model will be presented in Sect. 3. Section 4 is a description about the data preprocessing techniques used in this research. Section 5 presents the experiments set up and the results while Sect. 6 is devoted for some conclusion about the research.

2 Related Works

In agriculture and food industry, HSI can be used for detecting the unique spectral information of meat, fruits [4–6]. It can be used to identify, measure, and locate different materials as well as their chemical and physical properties. Machine learning, especially deep learning algorithms, which are popular for image processing, can be applied to these applications. Recently, deep learning algorithms have gained many attentions as they can solve many difficult problems [8–10]. For HSI, DNN are applied to classify food, the model achieves the best performance with a 94.4% overall classification accuracy independent of the

[1] https://www.shrimpalliance.com/fda-refuses-antibiotic-contaminated-shrimp-from-china-and-vietnam-in-july/.

state of the products, with high accuracy [5]. A research [5] presents an inclusive analysis of the performance of Hyperspectral Imaging for detecting adulteration in red-meat products. In [6], the developments and applications of HSI in the nondestructive assessment of fruits and vegetables are presented. Partial least squares regression is used as a multivariate method in calibration of spectroscopy data. In [4], deep learning algorithm is applied to visible and near-infrared HSI of shrimps for distinguishing the cleanness of shrimp during cold storage.

In food industry, shrimp is one of the rich in protein production, high quality food and the tasks of guaranteeing the quality and safety of s are crucial. In [4], the cleanness of shrimp during cold storage is investigated using visible light and near-infrared (VIS/NIR) hyperspectral images. Deep learning algorithm is applied to analyze the HSI for calculating the cleanness of shrimps. The stacked Autoencoders - Linear Regression algorithm achieves satisfactory total classification accuracy of 96.55% and 93.97% for freshness grade of shrimp in calibration (116 samples) and prediction (116 samples) sets, respectively. In [11], the authors aimed to develop an image-based method for detection of improperly deveined shrimps. A sequence of image processing techniques in this work is subjected before extracting significant parameters from gray scale images. Some parameters including shape measurements and pixel value measurements are drawn from the image histogram. Then, deveined shrimps were identified by two classification techniques: linear discriminant analysis and support vector machine (SVM). Despite the excellent capability of the HSI in food industries, there are still not many works applying HSI to shrimp productions.

In this paper, the classification of shrimps under limited number of HSI data cubes is presented. Our system includes the following steps: collecting, preprocessing and extracting data, then building a DNN model to classify these data into two classes (contaminated shrimps and clean shrimps). Due to limited a number of samples, the data augmentation approach in [4] is applied to enrich our training data. By extracting spectral information of HSI, the difference between clean shrimps and contaminated ones can be explored. These data will be used for detecting contaminated shrimps using a DNN model. The results shows that DNN can classify shrimps using small number of HSI data cube with high accuracy.

3 System Model

The system for detecting contaminated shrimps from their HSIs using deep neural network was shown in Fig. 1. Let the HSI data cube be $s = [s_{ijk}]$ which is three dimensional data matrix of size $H \times W \times F$, where H, W are the height and the width of the shrimp image in pixel, and F is the number of wave length bins representing the recordable bandwidth of the HSI machine. Here, i,j are the width and height indices of the shrimp image, and k is the wave length index starting 1 to 224 to represent the wavelength of the HSI from 400 nm to 1000 nm. Going together with each HSI is a RGB image of the same size. The meat parts of the shrimps are extracted. Segmentation is applied to the input

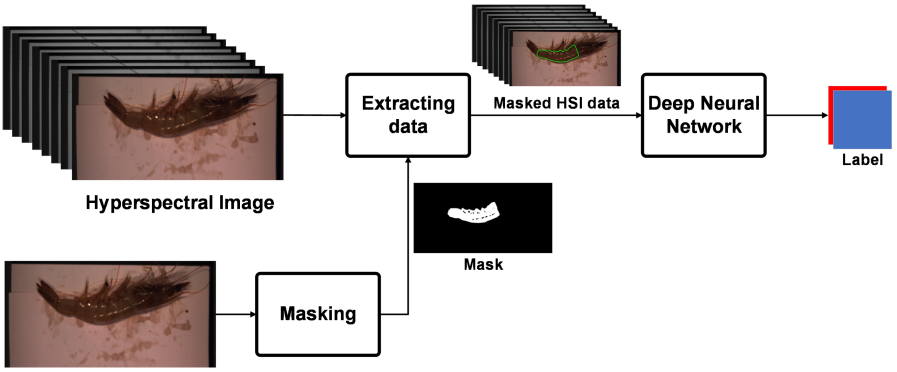

Fig. 1. System model for classifying using hyperspectral image, RGB image and deep neural network.

HSI data cubes to separate the shrimp image part and the background. Noise filtering techniques are applied to remove unwanted noise caused by the shooting environment. The denoised data is extracted and fed into the neural network. The training HSI data cubes labeled as "clean" and "contaminated" are used to finding the optimum weights of the DNN. After training, our system can be used to classify clean and contaminated shrimps.

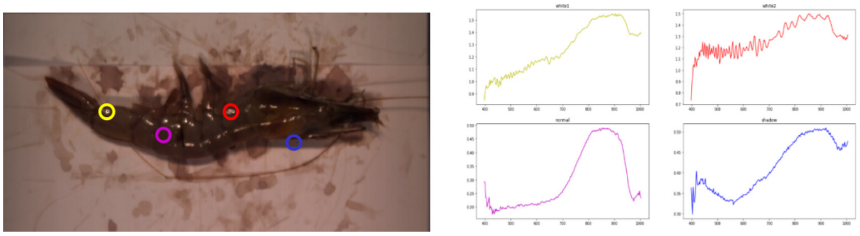

Fig. 2. Visualize noise data. (a) white noise (yellow and red), shadow of shrimp (blue), normal point (pink). (b) spectral data of fours points in (a) (Color figure online)

First, the useful part of data cube, i.e., the meat parts of the shrimps, is extracted in the data pre-processing phase. Figure 2(a) shows a shrimp image and Fig. 2(b) shows the hyper spectrum at four locations: good data area (marked as pink), white area (marked as yellow and red), shadow of the shrimp (marked as blue). It can be seen that the spectrum of the good data area has different properties compared to that of white area and shadows, especially in infrared regime. Due to the strong light condition in HSI machine, some parts of the shrimp image appear as white marks as the reflection from the light. As the marks are pure white, a simple threshold-based method can be applied to the data cube to exclude the white marks from the good data [12]. The background

of the images is also white, therefore, this method also can separate the shrimp and the background. Figure 3(a) shows the results of white area removal. The white marked and the background is removed from the image.

Fig. 3. Preprocessing and extracting data of shrimp from hyperspectral image. (a) our first mask which removes white noise and white background. (b) boundary of shrimp body after using Labelme. (c) the last mask achieved by combining our first mask (a) and boundary (b)

However, the data cube still mix the meat part of shrimp, the shrimp legs, and the shadow. The shrimp legs and the shadow part can be removed by the segmentation process. For focusing to the problem of shrimp classification, in this work, the data segmentation is performed manually with the associated RGB images to have good segmentation results. The shrimp images are segmented to extract only the body parts. As can be seen in Fig. 3(a), the boundary of shrimps should be created to avoid shrimp shadow generated by the light from the spectroscopy machine. Because impurities or chemical changes usually happens on shrimp bodies, only the bodies of shrimps where shrimps' flesh is concentrated is taken into account. Using the Labelme tool [13], a new boundary for shrimp is achieved as in Fig. 3(b). Combining the first mask and the boundary, a better mask as in Fig. 3(c) is produced.

Figure 4(a) shows the resulting hyperspectrum of several data cubes after extraction for clean shrimps (marked as blue) and contaminated shrimps (marked as red). The hyper spectrum curves of each HSI data cube are averaged from the hyperspectrum curves of every pixels belonging to the data cube. The average hyperspectrum can be calculated as

$$s_k = \frac{1}{HW} \sum_i \sum_j s_{ijk} \tag{1}$$

The HSI data cube now becomes the vector $x = [s_1, s_2, ..., s_F]$ of size F. This new data can be used to train the DNN to classify the clean shrimps and contaminated shrimps.

4 Data Preprocessing

4.1 Hyperspectral Data Visualization

In general, DNN can be applied to classify the two type of shrimps using processed HSI data. Usually, the required number of inputs for training a DNN can

be up to thousands. If the number of training data is not large enough, DNN can not learn correctly most of object features and this may lead to incorrect prediction.

Our data set includes 20 HSIs of clean shrimps and 15 HSIs of contaminated shrimps with size of HSIs 512×1024 and number of wavelength $F = 224$. Due to the limited number of shrimp HSI data cubes, data augmentation for HSI must be applied. In this work, the shrimp bodies' images are divided into smaller square areas. Let the size of the square be S, we can divide a shrimp HSI of size $H \times W \times F$ into many shrimp HSI images of size $S \times S \times F$ depending on the result of the segmentation process. Using (1) to the square images, we obtained a quite large data set of hyperspectrum vectors of size F used for classification process using neural network.

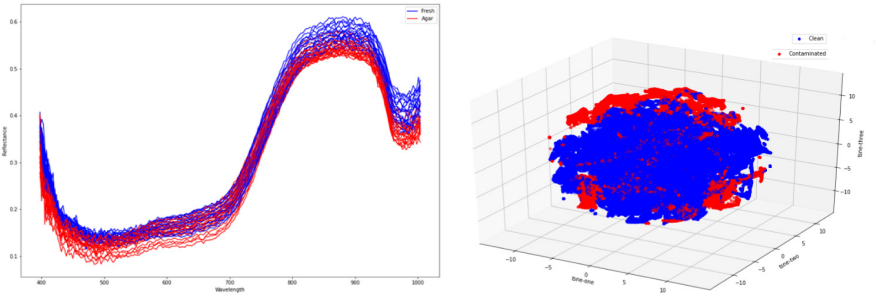

Fig. 4. t-SNE anlysis on shrimp's hyperspectrum. (a) mean spectra of each of two classes: contaminated shrimp (red) and clean shrimp (blue). (b) scatter plot 3D for contaminated shrimp class and clean shrimp class. (Color figure online)

As can be seen in Fig. 4(a), the spectrum curves of clean shrimps and contaminated shrimps are quite similar, making it difficult for classification. The spectrum of each pixel of data cubes for two types of shrimps are even more intermingled. Therefore, we apply a non-linear visualization technique to determine the possibility of classification. Recently, t-SNE has been popular for data visualization as it can reduces the high dimensional data set into 3-dimensional data set where the dissimilarity properties of two data set is preserved statistically [1]. Let the hyperspectral data set of some shrimp be $X = \{x_1, x_2, ..., x_N\}$, where N is the total number of hyperspectral data vectors calculated from (1) for all augmented data cubes. The t-SNE output is the data set $Y = \{y_1, y_2, ..., y_N\}$ of 3-dimensional data vectors. As such, the hyperspectral data of F dimensions can be visualized.

The perplexity parameter is set at 40 according to the recommendation of skLearn framework. To ensure the convergence of the Kullback-Leibler divergence loss function, the number of iterations is set at 400. Other parameters are set as default in sklearn.manifold.TSNE function of skLearn framework.

Figure 4(b) shows the best output of t-SNE in 3D coordinators. It can be seen that the data points corresponding to the contaminated shrimp (marked

as red) is in the outer sphere while the clean shrimp data points gathered in the inner sphere. Hence, it is possible to differentiate the contaminated shrimps from the clean ones. Due to the t-SNE property that the visualization results are non-deterministics, it can not be used for classification. In the following section, contaminated/clean shrimps classification using Deep Neural Network (DNN) is presented.

4.2 DNN for Classification

In this sub-section, we describe the deep learning model for classifying contaminated shrimps and clean shrimps. To the best of our knowledge, this is the first time that DNN has been applied to HSI imaging for contaminated shrimp detection.

Different dataset created by different sizes of window would affect the results of the model.

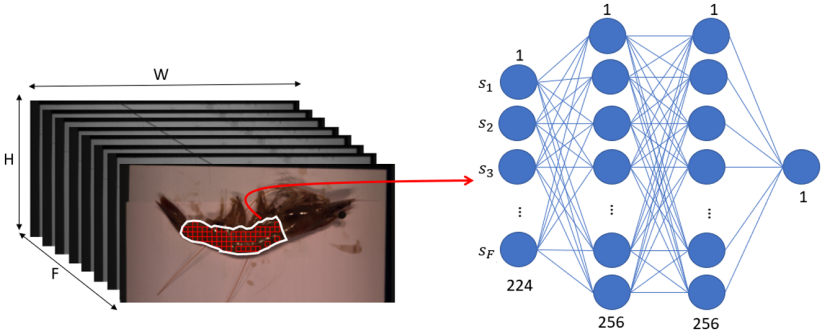

Fig. 5. Applying deep neural network in hyperspectral image with many size of window data.

A fully connected layers DNN with two hidden layers is used. Table 1 summarizes the specifications of the DNN model and Fig. 5 describes the DNN with shrimps' hyperspectral vectors as inputs. The input layer has 224 units corresponding to 224 spectral bin of the HSI and takes the HSI vector x as input. The output layer has 1 unit as the results is binary classification. The output is 1 if contaminated shrimp is detected and 0 if clean shrimp is detected. At each hidden layer, Rectified Linear Unit function (ReLU) [14] to non-linearity transformation are applied for accelerating the training processes. In the classification layer, i.e., output layer, the Sigmoid activation [15] is used.

For training the DNN, we use Adam algorithm [16] with the back-propagation algorithm for minimizing the loss function and updating the weight matrix and the bias vector of each layer. The binary cross entropy algorithm [17] is chosen as loss function:

$$J = -\frac{1}{M}\sum_{i=1}^{N}(z_i \times log(\hat{z}_i) + (1 - z_i) \times log(1 - \hat{z}_i)), \tag{2}$$

Table 1. Specifications of DNN model

Layer	No. unit	Activation function	Parameters
Input layer	224	-	-
Hidden layer 1	256	ReLU	57600
Hidden layer 2	256	ReLU	65792
Output layer	1	Sigmoid	257

where M is the batch size for each DNN's weight update, z_i is label of i^{th} data in the batch and $\hat{z}_i$ is the model prediction of i^{th} data.

5 Experiments and Results

5.1 DNN Setup and Metrics

These input data set X with their labels is divided into three sets: Training set (60%), Validating set (20%) and Testing set (20%). Training set is the input of DNN for learning, for estimating the parameters. Validating set is used to give an estimate of model skill while tuning DNN model's hyper-parameters. The testing set is used to evaluate model.

The learning rate of Adam algorithm is set at 0.001. The batch size $M = 128$ to have a good balance between accuracy and running time.

The metrics based on confusion matrix including accuracy, precision, recall, F1-score is used to evaluate the experimental results. The definition of the confusion matrix is shown in Table 2, where true positive (TP), true negative (TN), false positive (FP), and false negative (FN) are the number of correctly recognized contaminated shrimp, the number of correctly recognized clean shrimp, the number of incorrectly recognized clean shrimp, and the number of incorrectly recognized contaminated shrimp, respectively.

Accuracy, precision, recall, F1-score for evaluating the effectiveness of the DNN model can be calculated as follows

$$Accuracy = \frac{TP + TN}{TP + TN + FP + FN} \tag{3}$$

$$Precision = \frac{TP}{TP + FP} \tag{4}$$

Table 2. Confusion matrix

		Predicted	
		Contaminated shrimp	Clean shrimp
Real	Contaminated shrimp	TP	FN
	Clean shrimp	FP	TN

$$Recall = \frac{TP}{TP + FN} \tag{5}$$

$$F1 = \frac{2 \times Precision \times Recall}{Precision + Recall} \tag{6}$$

5.2 Results and Discussion

In the first experiments, we examine the effect of window size S on the training process of DNN. The window size under test are 1, 3, 5 and 8. In these training processes, early stopping is set as 20. Early stopping results are used for evaluate results on validating set. If the accuracy of validating set does not improve after 20 epochs, the training processes are interrupted. The accuracy and the loss of the training processes are shown in Fig. 6(a) and Fig. 6(b), respectively. All of the training processes converge and achieve reasonable training accuracy and loss after about 50 epochs. The training accuracy and loss of window size of 5 gains the highest results while that of window size 1 exhibits the worst values.

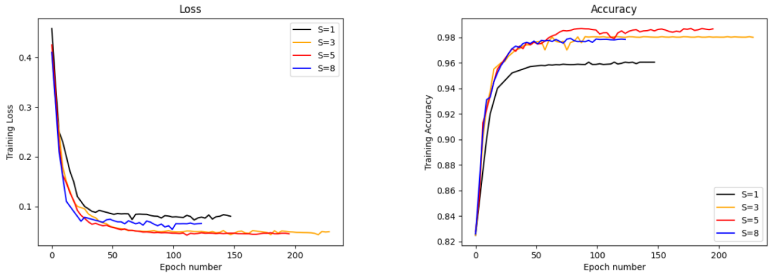

Fig. 6. The training process. (a) loss. (b) accuracy

Table 3 show the loss, accuracy, recall, precision and F1-score of experiments with different window size and number of data points. Note that, the number of data points does not reduce with square rate as the window size S increases. For having enough data points to train the DNN, for window size larger than 1, a sliding window technique is applied to sample the data. The influence of the window size on the accuracy and F1-score is also shown in Fig. 7. The losses are small enough to decide that the DNN model has converged. The other metrics shows that the DNN works well for all cases and the classification of contaminated shrimps and clean shrimps can be accomplished using DNN. The results also show that the data point of size 5×5 provides the best result. The accuracy is 98.11% and the F1-score is 94.29%. It is reasonable because the averaging of spectra in each window helps to reject several types of noise, such as salt-and-pepper noise. Furthermore, averaging over large size of windows may leads to feature loss.

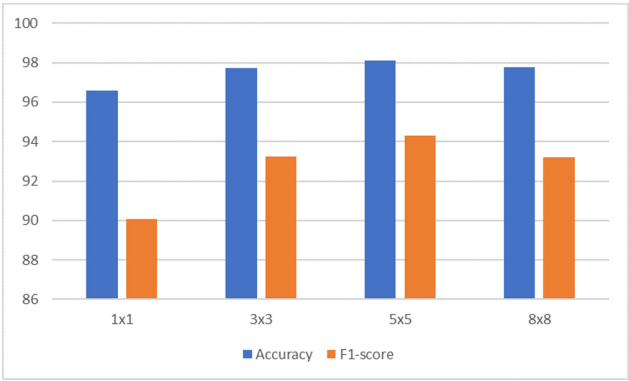

Fig. 7. The effect of window size on the accuracy and F1-score of DNN.

Table 3. Result for the window size of data task

Window size	No. data	Loss	Accuracy	Recall	Precision	F1-score
1×1	514639	0.0874	96.57	87.50	92.77	90.06
3×3	470472	0.0572	97.73	89.99	96.75	93.25
5×5	429665	0.0496	98.11	90.27	98.70	94.29
8×8	371163	0.0578	97.78	90.83	95.72	93.21

6 Conclusion

In this paper, we examine the possibility of contaminated/clean shrimps classification using Deep Learning with HSI data. Data visualization using t-SNE has shown that the classification is feasible. With only few HSI data samples, DNN successfully differentiate the contaminated shrimps and the clean ones with good F1 score. In the future, the better result might be achieved by the detection only contaminated part of shrimps.

Acknowledgement. We thank Minh Phu seafood corporation for providing hyperspectral imaging data and inspiring us to realize this work.

References

1. van der Maaten, L., Hinton, G.: Visualizing data using t-SNE. J. Mach. Learn. Res. **9**, 2579–2605 (2008)
2. Schelkanova, I., Pandya, A., Muhaseen, A., Saiko, G., Douplik, A.: 13 - early optical diagnosis of pressure ulcers. In: Igor, M. (ed.) Biophotonics for Medical Applications, pp. 347–375. Woodhead Publishing (2015)
3. Vasefi, F., MacKinnon, N., Farkas, D.L.: Chapter 16 - hyperspectral and multispectral imaging in dermatology. In: Hamblin, M.R., Avci, P., Gupta, G.K. (eds.) Imaging in Dermatology, pp. 187–201. Academic Press, Boston (2016)

4. Yu, X., Tang, L., Wu, X., Lu, H.: Nondestructive freshness discriminating of shrimp using visible/near-infrared hyperspectral imaging technique and deep learning algorithm. J. Food Anal. Methods **11**, 768–780 (2018)
5. Al-Sarayreh, M., Reis, M., Yan, W., Klette, R.: Detection of red-meat adulteration by deep spectral-spatial features in hyperspectral images. J. Imaging **4**, 63 (2018)
6. Li, X., Li, R., Wang, M., Liu, Y., Zhang, B., Zhou, J.C.: Hyperspectral imaging and their applications in the nondestructive quality assessment of fruits and vegetables (2017). https://doi.org/10.5772/intechopen.72250
7. Specim: Specim FX10 - user guide 1.0. Specim imaging Oy Ltd
8. Li, Y., Zhang, H., Xue, X., Jiang, Y., Shen, Q.: Deep learning for remote sensing image classification: a survey. In: Wiley Interdisciplinary Reviews: Data Mining and Knowledge Discovery, p. e1264 (May 2018). https://doi.org/10.1002/widm.1264
9. Wang, W., et al.: Medical image classification using deep learning. In: Chen, Y.-W., Jain, L.C. (eds.) Deep Learning in Healthcare. ISRL, vol. 171, pp. 33–51. Springer, Cham (2020). https://doi.org/10.1007/978-3-030-32606-7_3
10. Lu, Y.: Food image recognition by using convolutional neural networks (CNNs) (December 2016)
11. Thanasarn, N., Chaiprapat, S., Waiyakan, K., Thongkaew, K.: Automated discrimination of deveined shrimps based on grayscale image parameters. J. Food Process Eng. **42**, e13041 (2019). https://doi.org/10.1111/jfpe.13041
12. Sural, S., Qian, G., Pramanik, S.: Segmentation and histogram generation using the HSV color space for image retrieval. In: Proceedings of International Conference on Image Processing, vol. 2, pp. II-589 (February 2002). https://doi.org/10.1109/ICIP.2002.1040019
13. Russell, B., Torralba, A., Murphy, K., Freeman, W.: LabelMe: a database and web-based tool for image annotation. Int. J. Comput. Vis. **77**, 157–173 (2008). https://doi.org/10.1007/s11263-007-0090-8
14. Hahnloser, R., Sarpeshkar, R., Mahowald, M.A., Douglas, R.J., Seung, H.S.: Digital selection and analogue amplification coexist in a cortex-inspired silicon circuit. Nature **405**(6789), 947–951 (2000)
15. Han, J., Moraga, C.: The influence of the sigmoid function parameters on the speed of backpropagation learning. In: Mira, J., Sandoval, F. (eds.) IWANN 1995. LNCS, vol. 930, pp. 195–201. Springer, Heidelberg (1995). https://doi.org/10.1007/3-540-59497-3_175
16. Kingma, P., Lei Ba, J.: Adam: a method for stochastic optimization. arXiv:1412.6980v9 (2014)
17. Goodfellow, I., Bengio, Y., Courville, A.: Deep Learning. MIT Press, Cambridge (2016)